Hamstrings Contraction Regulates the Magnitude and Timing of the Peak ACL Loading During the Drop Vertical Jump in Female Athletes

Ryo Ueno,*†‡ PT, PhD, Alessandro Navacchia,†§ PhD, Nathan D. Schilaty,†‖¶ DC, PhD, Gregory D. Myer,#**††‡‡ PhD, Timothy E. Hewett,§§‖‖ PhD, and Nathaniel A. Bates,†‖ PhD
Investigation performed at the Mayo Clinic, Rochester, Minneapolis, Minnesota, USA

Background: Anterior cruciate ligament (ACL) injury reduction training has focused on lower body strengthening and landing stabilization. In vitro studies have shown that quadriceps forces increase ACL strain, and hamstring forces decrease ACL strain. However, the magnitude of the effect of the quadriceps and hamstrings forces on ACL loading and its timing during in vivo landings remains unclear.

Purpose: To investigate the effect and timing of knee muscle forces on ACL loading during landing.

Study Design: Descriptive laboratory study.

Methods: A total of 13 young female athletes performed drop vertical jump trials, and their movements were recorded with 3-dimensional motion capture. Lower limb joint motion and muscle forces were estimated with OpenSim and applied to a musculoskeletal finite element (FE) model to estimate ACL loading during landings. The FE simulations were performed with 5 different conditions that included/excluded kinematics, ground-reaction force (GRF), and muscle forces.

Results: Simulation of landing kinematics without GRF or muscle forces yielded an estimated median ACL strain and force of 5.1% and 282.6 N. Addition of GRF to kinematic simulations increased ACL strain and force to 6.8% and 418.4 N ($P < .05$). Addition of quadriceps force to kinematics + GRF simulations nonsignificantly increased ACL strain and force to 7.2% and 478.5 N. Addition of hamstrings force to kinematics + GRF simulations decreased ACL strain and force to 2.6% and 171.4 N ($P < .001$). Addition of all muscles to kinematics + GRF simulations decreased ACL strain and force to 3.3% and 195.1 N ($P < .001$). With hamstrings force, ACL loading decreased from initial contact (time of peak: 1-18 milliseconds) while ACL loading without hamstrings force peaked at 47 to 98 milliseconds after initial contact ($P = .024-.001$). The knee flexion angle increased from 20.9° to 73.1° within 100 milliseconds after initial contact.

Conclusion: Hamstrings activation had greater effect relative to GRF and quadriceps activation on ACL loading, which significantly decreased and regulated the magnitude and timing of ACL loading during in vivo landings.

Clinical Relevance: Clinical training should focus on strategies that influence increased hamstrings activation during landing to reduce ACL loads.

Keywords: knee; finite element; musculoskeletal; modeling; strain; landing

Injury reduction is the optimal concept to avoid the complications of extended rehabilitation, failure to return to sport, and high rates of second injury that are associated with anterior cruciate ligament (ACL) rupture.[1,16,38,44] Literature indicates that incidence of ACL injury can be mitigated across a population by interventions targeted at modifiable risk factors, such as neuromuscular control and movement biomechanics.[20,56] Specifically, implementation

of neuromuscular training programs that incorporate lower body strength, landing stabilization, core strength, agility, plyometrics, and balance[39] influence muscle activations in a manner that mitigates biomechanical risk factors associated with ACL injury during landing tasks.[17,18,39,49] However, the specific impacts of targeting muscular recruitment and strengthening strategies on ACL loading have not been well established owing to the difficulty of assessing direct ACL loads in vivo.

In vitro experimental testing indicates that quadriceps forces increase ACL loads, as opposed to hamstrings forces, which reduce ACL strain.[32,43,47] In quasi-static conditions,

400 N of quadriceps tension was shown to increase ACL strain by 3% to 5%.[43,47] This is consistent with an in vivo study that reported ACL strain increased with quasi-static quadriceps contraction.[4] Conversely, greater quadriceps tension decreased (or did not change) ACL loading during simulated in vitro landings.[15,30] These studies suggested that the response of ACL loading to quadriceps force would be different between quasi-static and dynamic conditions. The effect of muscle contractions on ACL loading during in vivo landing tasks remains unclear, as multiple interactions take place between dynamic kinematics, muscle forces, and ground-reaction force (GRF). Specifically, the magnitude of the effect of quadriceps and hamstrings forces on ACL loading and its timing during landing remains unexplored.

Musculoskeletal models are helpful, as they allow investigators to estimate in vivo muscle forces and ligament loading, which is not experimentally measurable.[24,28,35,36,51,53,55] A previous musculoskeletal modeling study revealed that hamstrings force is more effective at decreasing anterior tibial shear force during a drop vertical jump (DVJ) than quadriceps force at increasing it.[36] However, that study did not investigate ligament loading because ligamentous structures were not included in the model.

A validated knee joint model is necessary to provide physiologic knee ligament loading because generic material properties fail to account for the specimen-specific coupling of shape and structural properties.[34] Only some musculoskeletal modeling studies have reported ligament loading with validated material properties and a 6 degrees of freedom (DOF) knee joint, which is optimal for the accurate assessment of ligament loading.[24,28,35,48,55] Once a musculoskeletal model is validated, it can be used to simulate the individual effect of multiple factors, including kinematics, muscle forces, and/or GRF during landing.[34] A similar technique utilizing a validated model was used in previous studies to test other joints and tasks,[13,23,24,29,35,48] but ACL loading during a landing task has not been studied.

The purpose of this study was to employ a validated musculoskeletal model to test the individual effect of kinematics, GRF, and muscle forces on ACL loading during a simulated landing task. We hypothesized that isolated quadriceps force would increase ACL loading, whereas hamstrings would decrease ACL loading above and beyond the effect of quadriceps contributions during landing simulations.[15,30,57] Furthermore, because ACL injury occurs at 40 to 60 milliseconds after initial contact with anterior tibial translation,[3,26,27,37,52] we hypothesized that hamstrings would decrease ACL loading around this time range as an agonist of ACL. This would shift the time of peak ACL loading to the initial contact, at which time the knee flexion angle is at its minimum.[8]

METHODS

Experimental Testing

The experimental data collection for this study was previously described in detail.[53] In brief, 13 female high school volleyball players (mean age, 15.6 ± 1.6 years; mean height, 169.8 ± 5.6 cm; mean weight, 62.6 ± 5.2 kg) participated in this study. Each participant performed 3 DVJ trials from a 30 cm–high box. Individuals' 3-dimensional body positions and surface electromyography (EMG) data for the right leg were recorded during the DVJ using 35 reflective markers and a motion capture system and telemetry surface EMG system.[11] EMG was recorded for biceps femoris, semitendinosus, rectus femoris, vastus lateralis, vastus medialis, gastrocnemius medialis, hip adductors, and gluteus medius.

Computational Simulations

Sequential OpenSim[6] simulations and 2 finite element (FE) simulation steps were conducted to estimate ACL strain and force during landings. Joint kinematics and kinetics as well as muscle forces were estimated with OpenSim simulations and used as inputs to FE simulations. The individual effect of kinematics, GRF, and muscle forces were investigated by the inclusion/exclusion of these factors in separate simulations of the same motion task (Figure 1).

*Address correspondence to Ryo Ueno, PT, PhD, Department of Sport Science, University of Innsbruck, Fürstenweg 185, A-6020 Innsbruck, Austria (email: ryo.ueno@uibk.ac.at).

†Department of Orthopedic Surgery, Mayo Clinic, Rochester, Minnesota, USA.

‡Department of Sport Science, University of Innsbruck, Innsbruck, Austria.

§Smith & Nephew, San Clemente, California, USA.

∥Department of Physiology and Biomedical Engineering, Mayo Clinic, Rochester, Minnesota, USA.

¶Department of Physical Medicine & Rehabilitation, Mayo Clinic, Rochester, Minnesota, USA.

#Emory Sport Performance and Research Center, Flowery Branch, Georgia, USA.

**Emory Sports Medicine Center, Atlanta, Georgia, USA.

††Department of Orthopaedics, Emory University School of Medicine, Atlanta, Georgia, USA.

‡‡The Micheli Center for Sports Injury Prevention, Waltham, Massachusetts, USA.

§§Hewett Global Consulting, Rochester, Minnesota, USA.

∥∥The Rocky Mountain Consortium for Sports Research, Edwards, Colorado, USA.
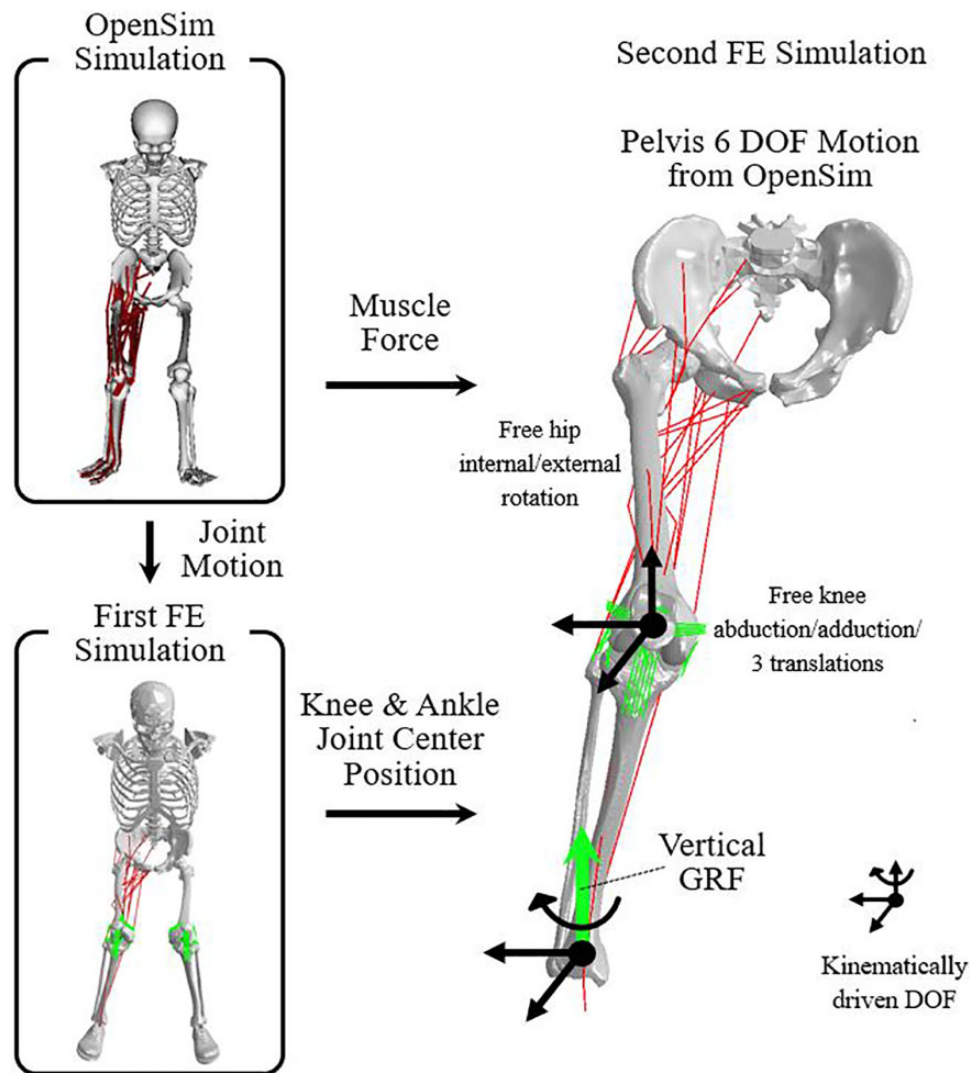
Figure 1. Workflow of the computational modeling to estimate ligament loading during the drop vertical jump, in which individual landing strategies were maintained. Joint motion and muscle forces were estimated using electromyography-informed optimization in OpenSim simulations. Joint motion was input to a first FE simulation to simulate landing with patient-specific kinematics and to obtain the trajectories of the knee and ankle joint centers. To simulate more physiologic knee joint mechanics, the joint center position was kinematically driven and muscle forces from OpenSim simulation were applied in the second FE simulation. Black arrows on the joint center indicate kinematically driven DOFs. Inferosuperior DOF on the ankle joint was unconstrained to apply vertical GRF, whereas rotation on the transverse plane was kinematically driven to track toe direction. The pelvis was kinematically driven according to the OpenSim inverse kinematics. This allowed hip internal/external rotation as well as knee abduction/adduction and the 3 translations of the knee to be unconstrained and dependent on muscle force, joint contact force, and GRF (see main text for more detailed description). DOF, degrees of freedom; FE, finite element; GRF, ground-reaction force.

OpenSim Simulations

Individual muscle forces were estimated in OpenSim as previously described.[53] Briefly, a generic musculoskeletal model[42] with additional DOFs added for knee abduction/adduction and internal/external rotation as well as additional hip external rotator muscles was scaled to the anthropometric parameters of each participant. These scaled models were used to calculate joint kinematics and muscle forces using EMG-informed direct collocation.[5] The objective function aimed to track participant-specific, experimentally measured EMG signals. In the musculoskeletal modeling step, 2 of 39 trials did not achieve the tolerance of muscle force optimization and were excluded from the analysis.

FE Simulations

A musculoskeletal FE model was created in Abaqus/Explicit (SIMULIA).[34] A generic model of the pelvis was

added to 1 of 4 previously developed and validated specimen-specific FE models of the knee (male, left leg in Navacchia et al[34]). The model included a 3-DOF ball joint at the hip, a 12-DOF knee joint, and a 1-DOF hinge joint at the ankle. The knee joint included specimen-specific bone and cartilage geometries and tibiofemoral and patellofemoral ligaments. The material properties of the ligaments including reference strain and stiffness were calibrated to match simulated kinematics and ACL strain with in vitro experimental testing measurements.[14,34] The 24 muscles (iliacus, psoas, 5 of adductors, 3 of gluteus maximus, 3 of gluteus medius, piriformis, 4 of hamstrings, 4 of quadriceps, 2 of gastrocnemius) that span the hip and knee joints were modeled as unidimensional connectors consistent with the OpenSim simulations.

The same landing tasks simulated with OpenSim were also simulated with the FE model. The FE landing simulation aimed to maintain physiologic mechanics at the knee and individual landing strategies such as knee-in, toe-out landing, which is determined by the knee and ankle joint center locations and toe direction in this study (the toe direction would not change during landing because of the friction). In the first FE simulation, pelvic, hip, knee, and ankle joint motions obtained from the OpenSim simulation were applied in the musculoskeletal FE model. The position in space of the knee joint center (midpoint between the medial and lateral knee condyles) and ankle joint center (midpoint between the medial and lateral malleoli) during landing were recorded. In the second FE simulation, the knee and ankle joint centers tracked their positions recorded in the first FE simulation, while rotational and translational DOF on the hip and knee joints remained unconstrained. The inferosuperior position of the ankle joint center was left free to transfer the ground force (vertical component only, as the other DOFs were kinematically driven) to the knee. In addition, a node on the ankle located 10 mm in front of the ankle joint center was kinematically driven in the mediolateral position to track the toe direction during landing. The muscle forces estimated in OpenSim and the vertical GRF were applied to each muscle and to the ankle, respectively.

This strategy was adopted to simulate the physiological knee joint mechanics while maintaining the individual landing strategies. Skin marker–based joint motions contain skin artifacts[31] and do not take into account the mechanical equilibrium of forces at the knee. Therefore, the knee joint motion obtained from OpenSim simulation in this study was not physiologic enough to assess ACL loading. The first FE simulation was necessary to obtain the joint center location of the FE model in the simulation of motion from OpenSim. The second FE simulation was separately conducted to satisfy mechanical equilibrium of forces at the knee joint. While hip flexion/extension, hip abduction/adduction, knee flexion/extension, and knee internal/external rotation were constrained owing to the kinematically driven knee and ankle joint centers, the positions of internal/external hip rotation, knee abduction/adduction, and translational DOF depended on muscle, ligament, contact forces, and GRF.

TABLE 1
Peak Values for Landing Kinematics[a]

Variable	Peak Value, deg
Knee flexion	73.1 (66.2 to 76.1)
Knee abduction	4.8 (3.8 to 6.0)
Knee internal rotation	21.4 (18.7 to 28.7)
Hip flexion	40.0 (34.5 to 44.9)
Hip adduction	−2.5 (−5.4 to −0.2)
Hip internal rotation	6.1 (2.4 to 10.2)
Lateral pelvic tilt	1.4 (−0.7 to 2.8)
Lateral lumber bending	2.3 (−0.7 to 3.9)

[a]Data are reported as median (interquartile range).

ACL strain and force were averaged and summed across the 4 modeled fibers (2 fibers each in the anteromedial and posterolateral bundles of the ACL), respectively. ACL strain was calculated as $100 \times (L - L_0)/L_0$, where L and L_0 are current length and reference length[9] (slack length determined by optimization in the validation study[34]), respectively. The FE simulation was conducted under 5 different conditions to sequentially investigate the individual effect of GRF and muscle forces on ACL loading with respect to the kinematics-only condition:

1. Kinematics condition (no application of GRF and muscle forces)
2. GRF condition (kinematics + GRF)
3. Quadriceps condition (kinematics + GRF + quadriceps)
4. Hamstrings condition (kinematics + GRF + hamstrings)
5. Normal condition (kinematics + GRF + all muscles)

Statistical Analysis

The Friedman test with post hoc Nemenyi multiple comparison test was used to examine the differences in ACL loading and peak time between the 5 conditions. Statistical tests were performed with R, package "PMCMR"[41] using jamovi V 1.2 (The jamovi project, https://www.jamovi.org). Statistical significance was set at $P < .05$.

RESULTS

The peak values for the landing kinematics are presented in Table 1, and Figure 2 shows the median ACL strain and force plotted across time for the 5 study conditions. For the kinematics condition, the median peak ACL strain and force were 5.1% (interquartile range [IQR], 4.3%-6.1%) and 282.6 N (IQR, 241.1-379.7 N), respectively (Table 2 and Figure 3, A and B). Significant increases in ACL strain and force were seen in the GRF condition compared with the kinematics condition, by 33% ($P = .017$) and 48% ($P = .011$), respectively. Nonsignificant increases in ACL strain and force were seen in the quadriceps condition compared with the GRF condition, by 5% ($P = .824$) and 14% ($P = .890$), respectively. ACL strain and force were
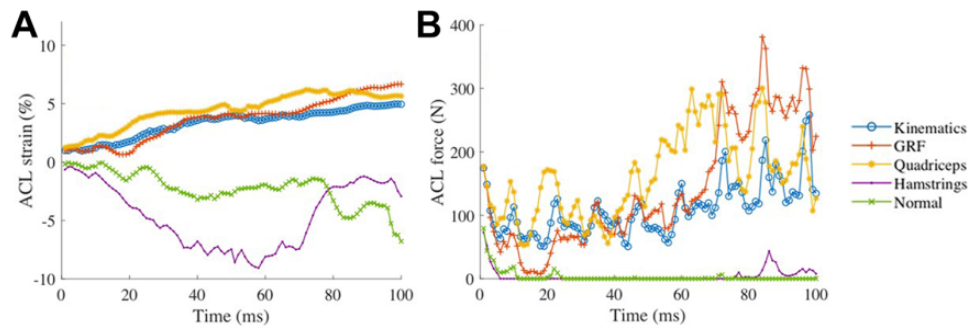
Figure 2. Median waveforms of ACL (A) strain and (B) force across time for the 5 different study conditions. Time zero indicates the time of initial contact with the ground. ACL, anterior cruciate ligament; GRF, ground-reaction force.

TABLE 2
Magnitude and Timing of Peak ACL Strain and Force by Study Condition[a]

	Kinematics	GRF	Quadriceps	Hamstrings	Normal
Peak ACL strain, %	5.1 (4.3 to 6.1)	6.8 (5.5 to 8.3)	7.2 (5.7 to 9.7)	2.6 (−1.8 to 3.6)	3.3 (−1.5 to 5.0)
Peak ACL force, N	282.6 (241.1 to 379.7)	418.4 (352.4 to 575.6)	478.5 (369.9 to 915.3)	171.4 (61.5 to 291.8)	195.1 (69.9 to 331.5)
Timing of peak ACL strain, ms	87 (45 to 99)	98 (73 to 100)	73 (58 to 97)	17 (1 to 87)	18 (1 to 56)
Timing of peak ACL force, ms	47 (7 to 97)	84 (56 to 85)	59 (46 to 80)	7 (1 to 85)	1 (1 to 45)

[a]Data are reported as median (interquartile range). ACL, anterior cruciate ligament; GRF, ground-reaction force.
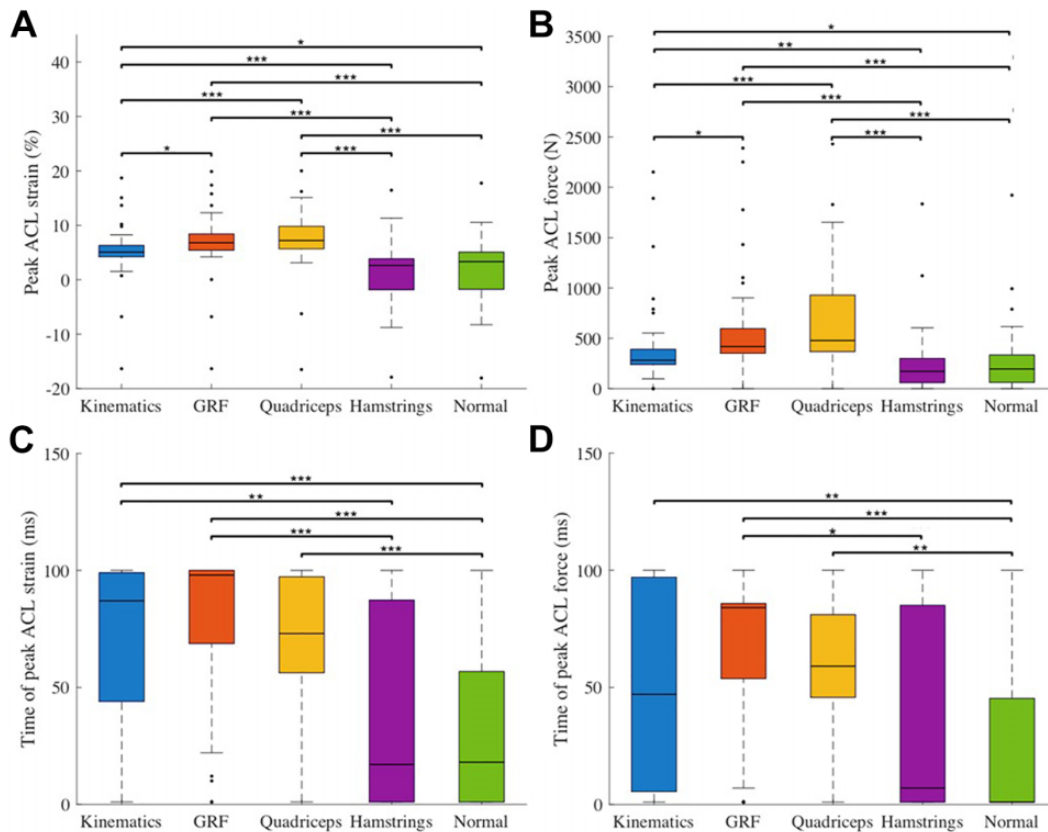

Figure 3. (A, B) Magnitude and (C, D) timing of peak anterior cruciate ligament (ACL) strain and force compared across the 5 study conditions. Dots indicate outliers. Asterisks indicate statistically significant differences: *$P < .05$; **$P < .01$; ***$P < .001$. GRF, ground-reaction force.

significantly decreased in the hamstrings condition compared with the GRF condition, by 62% and 59%, respectively ($P <$ .001 for both). Similarly, strain and force were significantly decreased in the normal condition compared with the GRF condition, by 51% and 54%, respectively ($P <$ .001 for both), as well as the quadriceps condition, by 45% and 41%, respectively ($P <$ .001 for both).

The timing of peak ACL strain and force after initial contact was significantly later in the kinematics, GRF, and quadriceps conditions compared with the hamstrings and normal conditions ($P =$ .024-.001) (Table 2 and Figure 3, C and D). The median knee flexion angle at initial contact was 20.9° (IQR, 15.9°-27.7°) and reached 73.1° (IQR, 66.2°-76.1°) at 100 milliseconds after initial contact.

DISCUSSION

To our knowledge, this was the first study to investigate the effect of muscle forces on ACL loading during simulations of in vivo landing with a validated musculoskeletal model. The hypothesis tested was that quadriceps force would increase ACL loading whereas hamstrings force would decrease ACL loading in this model. The hypothesis was partially supported, as the application of hamstrings force significantly decreased ACL loading during landing. Conversely, application of quadriceps force did not induce a statistically significant increase in ACL loading. Accordingly, relative to ACL loading, these observations indicate that the agonist effect of hamstrings contraction is larger than the antagonist effect of quadriceps during a landing task.

The results of the quadriceps condition did not directly support or contradict the previously cited in vitro literature that ACL loading remained unchanged when stiffness or preloading of quadriceps muscles was increased.[15,30] In a previous study,[30] the knee flexion angle was decreased because of higher quadriceps force. However, the FE simulation of the present study was designed to keep the knee flexion motion regardless of the quadriceps force or any other force. Therefore, the relationship between ACL strain, quadriceps force, and knee flexion angle found in the previous study[30] was not accounted for in the FE simulation. The kinematics + quadriceps condition without GRF was not tested in this study. ACL loading in such a condition is not expected to exceed the results of the quadriceps condition (kinematics + GRF + quadriceps) since the GRF significantly increased ACL strain when added to joint kinematics.

The result of the hamstrings condition was consistent with previous in vitro landing simulations.[57] The results of the normal condition indicated that the hamstrings compensated for most of the ACL loading that was incurred from GRF and quadriceps. These data indicate that ACL loading can be effectively regulated through hamstrings contraction, even when the applied hamstrings force is smaller (956.5 ± 232.0 N) than the quadriceps force (7278.4 ± 1308.1 N). This is consistent with a previous study that stated 55% of hamstrings force turned into posterior tibial force, whereas only 15% of quadriceps force turned

into anterior tibial shear force.[36] These findings provide evidence that hamstrings muscle activation contributes to protection of the ACL during landing tasks. At the same time, they indicate that isolated quadriceps force is not likely sufficient to induce ACL rupture on its own during landing.[7] Rather, the lack of hamstrings contraction combined with risky kinematics and GRF would be the most likely factors to induce ACL injury.

The time of peak ACL loading was delayed when hamstrings force was removed from the simulation. The hamstrings activation presented an increasing trend throughout the landing (see Ueno et al[53]), whereas the time of peak vertical GRF, knee abduction, internal tibial rotation, and anterior tibial translation, which induce higher ACL strain, were observed from 50 to 90 milliseconds (see Ueno et al[54] for more detailed knee kinematics). When hamstrings force was applied, 17 of 37 trials presented the peak ACL strain within 10 milliseconds after initial ground contact, where the knee flexion angle was at its minimum. These details indicate that kinematics, GRF, and quadriceps force strained the ACL from 50 to 90 milliseconds while hamstrings force canceled out these forces and shifted peak ACL loading to immediately after initial contact (0-10 ms) for the majority of trials. Note that peak ACL loading in the hamstrings condition was significantly smaller than in the other conditions. The time of peak ACL loading with hamstrings activation is consistent with previous fluoroscopic studies.[8,50] This result supports the fact that the hamstrings force regulates knee joint kinematics and ACL loading.

A limitation of this study was that the effect of the gastrocnemius was not tested. Fleming et al[10] reported that the gastrocnemius acts as an antagonist to the ACL as it pulls the femur backward relative to the tibia with an in vivo quasi-static study. Similarly, Navacchia et al[36] reported a musculoskeletal modeling study showing that the gastrocnemius induces anterior tibial shear force more than the quadriceps during landing. However, the similar effect was not simulated because of the constraints used in the FE analysis of this study. In addition, previous studies indicated that the gastrocnemius and quadriceps may contribute to stabilize the knee joint under a complexity of co-contraction.[2,25] These points should be improved and tested further in a future study.

Second, the magnitude of the effect of high-risk kinematics (such as higher knee abduction and internal tibial rotation with laterally leaned trunk) on ACL loading during landing remains unclear.[19,53] This concept should be examined in future studies to clarify the causal effects of individual landing strategies, including asymmetrical landing in the frontal plane and upright landing by changing landing posture.[21,45,46,53] However, these strategies will affect muscle force estimations. Therefore, muscle estimations must be reprocessed with respect to altered landing kinematics. Third, the effect of the anteroposterior and mediolateral components of GRF was not investigated since these DOFs were kinematically driven at the ankle to maintain individual landing strategies. Although the strategy used in this study maintains mechanical equilibrium without the application of horizontal GRFs, those ankle DOFs must be

unconstrained to address this limitation. However, the natural landing kinematics would be affected when kinematically driven ankle DOFs were unconstrained. Finally, the muscle force estimation would involve errors. Even though the EMG-informed method helped to account for the co-contraction of quadriceps and hamstrings,[36] surface EMG information would contain errors from crosstalk[33]; in addition, the estimation was not calibrated to be specific for patients as conducted in a previous study.[22,40] Uncoupled modeling between OpenSim and the FE model in this study would be another factor for the potential errors in the estimation of muscle force and subsequent ACL loads.[12,24,29,35,48]

CONCLUSION

The effect of quadriceps force on increasing ACL loads was smaller than the effect of GRF, whereas relatively small hamstrings force significantly decreased ACL loads during landing. ACL loading was effectively regulated by hamstrings force in a landing simulation model with kinematics, GRFs, and quadriceps co-contraction. The hamstrings muscle was a more influential agonist to ACL loading than any other input parameter was an antagonist. Clinicians should ensure appropriate hamstrings contraction and avoidance of risky kinematics and large GRF to reduce the relative risk of ACL injury.

ACKNOWLEDGMENT

REFERENCES

1. Ardern CL, Webster KE, Taylor NF, Feller JA. Return to the preinjury level of competitive sport after anterior cruciate ligament reconstruction surgery: two-thirds of patients have not returned by 12 months after surgery. *Am J Sports Med*. 2011;39(3):538-543.
2. Aune AK, Cawley PW, Ekeland A. Quadriceps muscle contraction protects the anterior cruciate ligament during anterior tibial translation. *Am J Sports Med*. 1997;25(2):187-190.
3. Bates NA, Schilaty ND, Ueno R, Hewett TE. Timing of strain response of the ACL and MCL relative to impulse delivery during simulated landings leading up to ACL failure. *J Appl Biomech*. Published online April 22, 2020. doi:10.1123/jab.2019-0308
4. Beynnon BD, Fleming BC. Anterior cruciate ligament strain in-vivo: a review of previous work. *J Biomech*. 1998;31(6):519-525.
5. De Groote F, Pipeleers G, Jonkers I, et al. A physiology based inverse dynamic analysis of human gait: potential and perspectives. *Comput Methods Biomech Biomed Engin*. 2009;12(5):563-574.
6. Delp SL, Anderson FC, Arnold AS, et al. OpenSim: open-source software to create and analyze dynamic simulations of movement. *IEEE Trans Biomed Eng*. 2007;54(11):1940-1950.
7. Domire ZJ, Boros RL, Hashemi J. An examination of possible quadriceps force at the time of anterior cruciate ligament injury during landing: a simulation study. *J Biomech*. 2011;44(8):1630-1632.
8. Englander ZA, Baldwin EL, Smith WAR, Garrett WE, Spritzer CE, DeFrate LE. In vivo anterior cruciate ligament deformation during a single-legged jump measured by magnetic resonance imaging and high-speed biplanar radiography. *Am J Sports Med*. 2019;47(13):3166-3172.
9. Fleming BC, Renstrom PA, Beynnon BD, et al. The effect of weight-bearing and external loading on anterior cruciate ligament strain. *J Biomech*. 2001;34(2):163-170.
10. Fleming BC, Renstrom PA, Ohlen G, et al. The gastrocnemius muscle is an antagonist of the anterior cruciate ligament. *J Orthop Res*. 2001;19(6):1178-1184.
11. Ford KR, Myer GD, Schmitt LC, Uhl TL, Hewett TE. Preferential quadriceps activation in female athletes with incremental increases in landing intensity. *J Appl Biomech*. 2011;27(3):215-222.
12. Halloran JP, Ackermann M, Erdemir A, van den Bogert AJ. Concurrent musculoskeletal dynamics and finite element analysis predicts altered gait patterns to reduce foot tissue loading. *J Biomech*. 2010;43(14):2810-2815.
13. Halloran JP, Erdemir A. Adaptive surrogate modeling for expedited estimation of nonlinear tissue properties through inverse finite element analysis. *Ann Biomed Eng*. 2011;39(9):2388-2397.
14. Harris MD, Cyr AJ, Ali AA, et al. A combined experimental and computational approach to subject-specific analysis of knee joint laxity. *J Biomech Eng*. 2016;138(8):0810041-0810048. doi:10.1115/1.4033882
15. Hashemi J, Breighner R, Jang TH, Chandrashekar N, Ekwaro-Osire S, Slauterbeck JR. Increasing pre-activation of the quadriceps muscle protects the anterior cruciate ligament during the landing phase of a jump: an in vitro simulation. *Knee*. 2010;17(3):235-241.
16. Hewett TE, Bates NA. Preventive biomechanics: a paradigm shift with a translational approach to injury prevention. *Am J Sports Med*. 2017;45(11):2654-2664.
17. Hewett TE, Ford KR, Xu YY, Khoury J, Myer GD. Effectiveness of neuromuscular training based on the neuromuscular risk profile. *Am J Sports Med*. 2017;45(9):2142-2147.
18. Hewett TE, Ford KR, Xu YY, Khoury J, Myer GD. Utilization of ACL injury biomechanical and neuromuscular risk profile analysis to determine the effectiveness of neuromuscular training. *Am J Sports Med*. 2016;44(12):3146-3151.
19. Hewett TE, Myer GD. The mechanistic connection between the trunk, hip, knee, and anterior cruciate ligament injury. *Exerc Sport Sci Rev*. 2011;39(4):161-166.
20. Hewett TE, Myer GD, Ford KR, Paterno MV, Quatman CE. Mechanisms, prediction, and prevention of ACL injuries: cut risk with three sharpened and validated tools. *J Orthop Res*. 2016;34(11):1843-1855.
21. Hewett TE, Torg JS, Boden BP. Video analysis of trunk and knee motion during non-contact anterior cruciate ligament injury in female athletes: lateral trunk and knee abduction motion are combined components of the injury mechanism. *Br J Sports Med*. 2009;43(6):417-422.
22. Hoang HX, Diamond LE, Lloyd DG, Pizzolato C. A calibrated EMG-informed neuromusculoskeletal model can appropriately account for muscle co-contraction in the estimation of hip joint contact forces in people with hip osteoarthritis. *J Biomech*. 2019;83:134-142.
23. Hume DR, Navacchia A, Ali AA, Shelburne KB. The interaction of muscle moment arm, knee laxity, and torque in a multi-scale musculoskeletal model of the lower limb. *J Biomech*. 2018;76:173-180.
24. Hume DR, Navacchia A, Rullkoetter PJ, Shelburne KB. A lower extremity model for muscle-driven simulation of activity using explicit finite element modeling. *J Biomech*. 2019;84:153-160.
25. Klyne DM, Keays SL, Bullock-Saxton JE, Newcombe PA. The effect of anterior cruciate ligament rupture on the timing and amplitude of gastrocnemius muscle activation: a study of alterations in EMG measures and their relationship to knee joint stability. *J Electromyogr Kinesiol*. 2012;22(3):446-455.
26. Koga H, Nakamae A, Shima Y, et al. Mechanisms for noncontact anterior cruciate ligament injuries: knee joint kinematics in 10 injury situations from female team handball and basketball. *Am J Sports Med*. 2010;38(11):2218-2225.

27. Krosshaug T, Nakamae A, Boden BP, et al. Mechanisms of anterior cruciate ligament injury in basketball: video analysis of 39 cases. *Am J Sports Med*. 2007;35(3):359-367.

28. Lenhart RL, Kaiser J, Smith CR, Thelen DG. Prediction and validation of load-dependent behavior of the tibiofemoral and patellofemoral joints during movement. *Ann Biomed Eng*. 2015;43(11):2675-2685.

29. Li J. Development and validation of a finite-element musculoskeletal model incorporating a deformable contact model of the hip joint during gait. *J Mech Behav Biomed Mater*. 2021;113:104136.

30. Lipps DB, Oh YK, Ashton-Miller JA, Wojtys EM. Effect of increased quadriceps tensile stiffness on peak anterior cruciate ligament strain during a simulated pivot landing. *J Orthop Res*. 2014;32(3):423-430.

31. Lu T-W, O'Connor JJ. Bone position estimation from skin marker coordinates using global optimisation with joint constraints. *J Biomech*. 1999;32(2):129-134.

32. Markolf KL, Gorek JF, Kabo JM, Shapiro MS. Direct measurement of resultant forces in the anterior cruciate ligament. An in vitro study performed with a new experimental technique. *J Bone Joint Surg Am*. 1990;72(4):557-567.

33. Mesin L. Crosstalk in surface electromyogram: literature review and some insights. *Phys Eng Sci Med*. 2020;43(2):481-492.

34. Navacchia A, Bates NA, Schilaty ND, Krych AJ, Hewett TE. Knee abduction and internal rotation moments increase ACL force during landing through the posterior slope of the tibia. *J Orthop Res*. 2019; 37(8):1730-1742.

35. Navacchia A, Hume DR, Rullkoetter PJ, Shelburne KB. A computationally efficient strategy to estimate muscle forces in a finite element musculoskeletal model of the lower limb. *J Biomech*. 2019;84:94-102.

36. Navacchia A, Ueno R, Ford KR, DiCesare CA, Myer GD, Hewett TE. EMG-informed musculoskeletal modeling to estimate realistic knee anterior shear force during drop vertical jump in female athletes. *Ann Biomed Eng*. 2019;47(12):2416-2430.

37. Olsen OE, Myklebust G, Engebretsen L, Bahr R. Injury mechanisms for anterior cruciate ligament injuries in team handball: a systematic video analysis. *Am J Sports Med*. 2004;32(4):1002-1012.

38. Paterno MV, Rauh MJ, Schmitt LC, Ford KR, Hewett TE. Incidence of second ACL injuries 2 years after primary ACL reconstruction and return to sport. *Am J Sports Med*. 2014;42(7):1567-1573.

39. Petushek EJ, Sugimoto D, Stoolmiller M, Smith G, Myer GD. Evidence-based best-practice guidelines for preventing anterior cruciate ligament injuries in young female athletes: a systematic review and meta-analysis. *Am J Sports Med*. 2019;47(7):1744-1753.

40. Pizzolato C, Lloyd DG, Sartori M, et al. CEINMS: a toolbox to investigate the influence of different neural control solutions on the prediction of muscle excitation and joint moments during dynamic motor tasks. *J Biomech*. 2015;48(14):3929-3936.

41. Pohlert T. *PMCMR: Calculate Pairwise Multiple Comparisons of Mean Rank Sums*. 2018. https://cran.r-project.org/web/packages/PMCMR/PMCMR.pdf

42. Rajagopal A, Dembia CL, DeMers MS, Delp DD, Hicks JL, Delp SL. Full-body musculoskeletal model for muscle-driven simulation of human gait. *IEEE Trans Biomed Eng*. 2016;63(10):2068-2079.

43. Renström P, Arms SW, Stanwyck TS, Johnson RJ, Pope MH. Strain within the anterior cruciate ligament during hamstring and quadriceps activity. *Am J Sports Med*. 1986;14(1):83-87.

44. Schilaty ND, Nagelli C, Bates NA, et al. Incidence of second anterior cruciate ligament tears and identification of associated risk factors from 2001 to 2010 using a geographic database. *Orthop J Sports Med*. 2017;5(8):2325967117724196.

45. Shimokochi Y, Ambegaonkar JP, Meyer EG. Changing sagittal-plane landing styles to modulate impact and tibiofemoral force magnitude and directions relative to the tibia. *J Athl Train*. 2016;51(7):669-681.

46. Shimokochi Y, Ambegaonkar JP, Meyer EG, Yong S, Sandra L. Changing sagittal plane body position during single-leg landings influences the risk of non-contact anterior cruciate ligament injury. *Knee Surg Sports Traumatol Arthrosc*. 2013;21(4):888-897.

47. Shimokochi Y, Shultz SJ. Mechanisms of noncontact anterior cruciate ligament injury. *J Athl Train*. 2008;43(4):396-408.

48. Shu L, Yamamoto K, Yao J, et al. A subject-specific finite element musculoskeletal framework for mechanics analysis of a total knee replacement. *J Biomech*. 2018;77:146-154.

49. Sugimoto D, Myer GD, Foss KDB, Hewett TE. Specific exercise effects of preventive neuromuscular training intervention on anterior cruciate ligament injury risk reduction in young females: meta-analysis and subgroup analysis. *Br J Sports Med*. 2015;49(5): 282-289.

50. Taylor K, Terry M, Utturkar G, et al. Measurement of in vivo anterior cruciate ligament strain during dynamic jump landing. *J Biomech*. 2011;44(3):365-371.

51. Ueno R, Ishida T, Yamanaka M, et al. Quadriceps force and anterior tibial force occur obviously later than vertical ground reaction force: a simulation study. *BMC Musculoskelet Disord*. 2017;18(1):467.

52. Ueno R, Navacchia A, Bates NA, Schilaty ND, Krych AJ, Hewett TE. Analysis of internal knee forces allows for the prediction of rupture events in a clinically relevant model of anterior cruciate ligament injuries. *Orthop J Sports Med*. 2020;8(1):2325967119893758.

53. Ueno R, Navacchia A, DiCesare CA, et al. Knee abduction moment is predicted by lower gluteus medius force and larger vertical and lateral ground reaction forces during drop vertical jump in female athletes. *J Biomech*. 2020;103:109669.

54. Ueno R, Navacchia A, Schilaty ND, Myer GD, Hewett TE, Bates NA. Anterior cruciate ligament loading increases with pivot-shift mechanism during asymmetrical drop vertical jump in female athletes. *Orthop J Sports Med*. 2021;9(3):2325967121989095.

55. Van Rossom S, Wesseling M, Smith CR, et al. The influence of knee joint geometry and alignment on the tibiofemoral load distribution: a computational study. *Knee*. 2019;26(4):813-823.

56. Webster KE, Hewett TE. Meta-analysis of meta-analyses of anterior cruciate ligament injury reduction training programs. *J Orthop Res*. 2018;36(10):2696-2708.

57. Withrow TJ, Huston LJ, Wojtys EM, Ashton-Miller JA. Effect of varying hamstring tension on anterior cruciate ligament strain during in vitro impulsive knee flexion and compression loading. *J Bone Joint Surg Am*. 2008;90(4):815-823.